Nitrogen removal via nitrite in a partial nitrification sequencing batch biofilm reactor treating high strength ammonia wastewater and its greenhouse gas emission

Dong Wei [a], Keyi Zhang [a], Huu Hao Ngo [b], Wenshan Guo [b], Siyu Wang [a], Jibin Li [a], Fei Han [a], Bin Du [a *], Qin Wei [c]

[a] *School of Resources and Environment, University of Jinan, Jinan 250022, PR China*

[b] *School of Civil and Environmental Engineering, University of Technology Sydney, Broadway, NSW 2007, Australia*

c Key Laboratory of Chemical Sensing & Analysis in Universities of Shandong, School of Chemistry and Chemical Engineering, University of Jinan, Jinan 250022, PR China

Abstract

In present study, the feasibility of partial nitrification (PN) process achievement and its greenhouse gas emission were evaluated in a sequencing batch biofilm reactor (SBBR). After 90 days' operation, the average effluent NH_4^+-N removal efficiency and nitrite accumulation rate of PN-SBBR were high of 98.2% and 87.6%, respectively. Both polysaccharide and protein contents were reduced in loosely bound extracellular polymeric substances (LB-EPS) and tightly bound EPS (TB-EPS) during the achievement of PN-biofilm. Excitation-emission matrix spectra implied that aromatic protein-like, tryptophan protein-like and humic acid-like substances were the main compositions of both kinds of EPS in seed sludge and PN-biofilm. According to

* Corresponding author. Tel: +86 531 8276 7370; fax: +86 531 8276 7370.
E-mail address: dubin61@gmail.com (B. Du)

typical cycle, the emission rate of CO_2 had a much higher value than that of N_2O, and their total amounts per cycle were 67.7 and 16.5 mg, respectively. Free ammonia (FA) played a significant role on the inhibition activity of nitrite-oxidizing bacteria and the occurrence of nitrite accumulation.

Keywords: Sequencing batch biofilm reactor; Partial nitrification; Extracellular polymeric substances (EPS); Excitation-emission matrix (EEM); Greenhouse gas emission.

1. Introduction

Biological nitrification-denitrification is typically utilized for nitrogen removal through two individual sequential processes: aerobic nitrification with the terminal conversion of NH_4^+-N to NO_3^--N and the subsequent anoxic denitrification with the conversion of NO_3^--N to molecular nitrogen (Adav et al., 2009). Recently, much attention has been paid to partial nitrification (PN) via nitrite process as a novel concept of BNR process. It theoretically saves approximately 25% of oxygen supply for nitrification, 40% of organic carbon as electron donor for denitrification and achieves a lower sludge production (Peng and Zhu, 2006). To date, PN process has been successfully applied for wastewater treatment containing high-nitrogen concentration or low carbon/nitrogen (C/N) ratio, such as municipal wastewater, landfill leachate and anaerobic sludge digester liquor etc (Ge et al., 2014; Qiao et al., 2008; Wang et al., 2010).

The main influencing factors to achieve and maintain PN process are including

dissolved oxygen (DO), pH value, sludge retention time (SRT), free ammonia (FA) and free nitrous acid (FNA) etc (Wei et al., 2015a). Till now, most of partial nitrification processes are reported by using synthetic wastewater as substrate under well-controlled laboratory-scale activated sludge reactors (Chen et al., 2016). However, little information is available for the achievement and maintenance of PN via nitrite through a biofilm system. Compared to suspended-growth activated sludge, biofilm system has the ability to provide different sub-zones for various types of bacteria, and therefore protect the slow-growing nitrifying bacteria from washout in the competition of heterotrophic bacteria (Yin et al., 2015). Therefore, various biofilm systems, such as sequencing batch biofilm reactor (SBBR), moving bed biofilm reactor (MBBR) and fixed bed biofilm reactor (FBBR) etc, are increasingly being applied for treating various municipal and industrial nitrogen-containing wastewaters (Gilbert et al., 2014; Jin et al., 2012; Zhang et al., 2016). Especially, it is evident that the degradation of pollutants largely depends on the amount and activity of microorganisms, which is attached onto the solid surface of carrier for biofilm formation in the presence of extracellular polymeric substances (EPS) (Czaczyk and Myszka, 2007; Li et al., 2016). Microbial EPS likely have a dynamic double-layered structure of loosely bound EPS (LB-EPS) diffused from the tightly bound EPS (TB-EPS) that surround the cells (Zhao et al., 2015). Moreover, the two kinds of EPS fractions play different roles in maintaining the sludge floc structure and functions (Liu et al., 2010). However, there is still a lack of destructive research to evaluate the changes of EPS in a PN-biofilm achievement, and thus, the major components of

64 double-layered EPS have not been characterized.

65 Additionally, biological wastewater treatment is recognized as one of the major
66 sources of greenhouse gas (GHG) emissions, particularly carbon dioxide (CO_2) and
67 nitrous oxide (N_2O), causing a major challenge to global climate (Kong et al., 2016).
68 It is well reported that CO_2 and N_2O can be produced from the processes of organic
69 matter degradation and biological nitrogen removal, respectively. Especially, N_2O has
70 about 300 times higher global warming potential than that of CO_2. As a by-product
71 and intermediate product, N_2O emission from biological wastewater treatment is
72 influenced by various operational parameters, including DO concentration, nitrite,
73 COD/N, temperature and toxic compounds etc (Kampschreur et al., 2009). In
74 particular, nitrite accumulation was considered to be a major parameter for affecting
75 the emission of N_2O in both nitrification and denitrification stages, and therefore
76 mitigate the environmental benefits of PN process (Wei et al., 2014a). Therefore, it is
77 desirable to evaluate the GHG emissions in PN biofilm system in order to provide a
78 better understanding on the basis of PN process.

79 In present study, the feasibility of PN process achievement in a SBBR was
80 evaluated treating high strength ammonia wastewater. For more detailed insights, the
81 changes of LB-EPS and TB-EPS were qualitatively and quantitatively analyzed by
82 using chemical and fluorescence spectroscopic approaches during the PN-biofilm
83 formation. After the PN-SBBR achieving stable operation, the productions of CO_2 and
84 N_2O were carried out to evaluate the behavior of GHG emissions from wastewater
85 treatment through PN process. The acquired results would help us to fully reveal

PN-biofilm process by considering the point of GHG production.

2. Materials and methods

2.1 SBBR system and operational procedure

Fig. S1 shows the schematic diagram of the lab-scale SBBR used in present study, which was made of plexiglas with a working volume of 3.4 L (12 cm in diameter and 30 cm in height) at room temperature (25-27 ^{o}C). The SBBR was filled with 40% cylindrical bio-carriers (K3, plastic media), and each carrier with 25 mm in diameter and 12 mm in height, respectively. The specific surface area and bulk density of each carrier were 500 m^2/m^3 and 110 kg/m^3, respectively. Influent wastewater was prepared in a storage tank (60 L) and introduced to the bottom of the reactor through a water pump. Air was supplied at the bottom of reactor by using an air pump. The reactor was automatically operated through a time controller.

The anoxic-aerobic SBBR was sequentially operated at a cycle of 480 min, consisting of 5 min influent, 85 min anoxic phase, 360 min aerobic reaction, 20 min settling and 10 min effluent and idle. Electromagnetic stirrer was used as the mixing method to keep the suspension of sludge during anoxic and aerobic phases. The reactor was operated with a volumetric exchange ratio of 50%, resulting in hydraulic retention time (HRT) of 16 h. Activated sludge was taken from a plant treating soy protein wastewater as the inoculation of biofilm system. The plant was located at Shandong province in China treating high strength ammonia wastewater. The sludge retention time (SRT) and nitrogen loading rate of plant were about 20 day and 0.15 kg NH_4^+-N/(m^3·day), respectively. The initial mixed liquor suspended solids (MLSS)

concentration in the reactor was 3.0 g/L.

2.2 Synthetic wastewater

The compositions of synthetic wastewater were used in the experiment as follows: chemical oxygen demand (COD, as sodium acetate), 600 mg/L; NH_4^+-N (as ammonium chloride), 200 mg/L; K_2HPO_4, 112 mg/L; $CaCl_2$, 40 mg/L; $MgSO_4 \cdot 2H_2O$, 20 mg/L; $FeSO_4 \cdot 2H_2O$, 20 mg/L and trace element solution 1.0 ml/L. The composition of the trace mineral solution was as follows: H_3BO_3 0.05 g/L, $ZnCl_2$ 0.05 g/L, $CuCl_2$ 0.03 g/L, $MnSO_4 \cdot H_2O$ 0.05 g/L, $(NH_4)_6MoO_{24} \cdot 4H_2O$ 0.05 g/L, $AlCl_3$ 0.05 g/L, $CoCl_2 \cdot 6H_2O$ 0.05 g/L, $NiCl_2$ 0.05 g/L. The ratio of bicarbonate to NH_4^+-N was kept above 8.0 mg/mg to ensure the growth requirements of nitrifying bacteria, as similarly reported by Shi et al (2009). As a reslut, the influent pH values of wastewater were controlled between 8.0 and 8.5.

2.3 EPS extraction and spectra analysis

A heating method was used to extract the double-layered EPS from seed sludge and biofilm, including loosely bound EPS (LB-EPS) and tightly bound EPS (TB-EPS), and the detailed procedure could be found in the previous literature (Li and Yang, 2007). 3D-EEM spectra were obtained by using a fluorescence luminescence spectrometer (LS-55, Perkin-Elmer Co., USA). EEM spectra were gathered with scanning emission (Em) spectra from 280 to 550 nm at 0.5 nm increments by varying the excitation (Ex) wavelength from 200 to 400 nm at 10 nm increments. Synchronous fluorescence spectra of EPS samples were measured by ranging the excitation wavelengths from 250-550 nm with a constant offset ($\Delta\lambda$) of 60 nm. The

width of the Ex/Em slit and scanning speed were set to 5.0 nm and 1200 nm/min for all the fluorescence measurements, respectively.

2.4 Analytical methods

NH_4^+-N, NO_2^--N and NO_3^--N were analyzed in accordance with their respective standard methods (APHA, 2005). The pH and DO values were monitored by using on-line probes (3420i, WTW Company, Germany). The polysaccharide (PS) and protein (PRO) contents were measured by using phenol-sulphuric acid method and modified Lowry method, and glucose and bovine serum albumin (BSA) were used as the respective standards, respectively.

During stable typical cycle, N_2 and air were supplied into the PN-SBBR throughout the anoxic and aerobic phases, and the off-gases were collected into the gasbags to quantify the emission amounts of N_2O and CO_2. N_2O and CO_2 concentrations were measured by using a gas chromatography (7890B, Agilent Technologies, USA), and the detailed method could be found in the previous literature (Hu et al., 2011).

The nitrite accumulation ratio (NAR) of the reactor was calculated according to the following equation (Eq. (1)):

$$NAR(\%)=\frac{NO_2^-\text{-N}}{NO_2^-\text{-N}+NO_3^-\text{-N}}\times 100\% \quad (1)$$

The FA and FNA concentrations in the reactor could be calculated by using the following expression (Eq. (3) and Eq. (4)) reported by Ford et al. (1980):

$$\mathrm{FA}\ (mg/L) = \frac{17}{14} \times \frac{[NH_4 \cdot N] \times 10^{\mathrm{pH}}}{\exp[6334/(273+T)] + 10^{\mathrm{pH}}} \quad (2)$$

$$\mathrm{FNA}\ (mg/L) = \frac{46}{14} \times \frac{[NO_2^- \cdot N]}{\exp[-2300/(273+T)] \times 10^{\mathrm{pH}}} \quad (3)$$

3. Results and discussion

3.1 Achievement and maintenance of PN-SBBR

The SBBR was successively operated for more than 90 days for biofilm formation and nitrite accumulation. As shown in Fig. 1A, the seed sludge in the reactor quickly adapted to the influent nitrogen-rich wastewater, and NH_4^+-N removal efficiency generally increased to 99.4% in the start-up period (days 1-6). Afterwards, the average NH_4^+-N removal efficiency in the effluent was high of 98.2% throughout the rest period of experiment (days 7-90, n=32), and the average effluent NH_4^+-N concentration was less than 5 mg/L. Although the influent water quality had some fluctuation, the reactor still had an excellent nitrification performance for treating the synthetic high strength ammonia wastewater, suggesting that the biofilm system had a strong adaptability to the unstable influent substrate concentrations. Borghei and Hosseini (2005) also found that MBBR had a good resistance to the toxic shock loading and the reactor returned to steady state condition within only two or three cycles of retention time.

Correspondingly, a gradual increase of effluent NAR was observed along with the significant increase of NH_4^+-N removal efficiency in the start-up of PN system. Afterwards, the effluent NO_2^--N and NO_3^--N concentrations were average at 62.8 and 8.83 mg/L (days 64-90, n=10), respectively. As a result, the effluent NAR was average at 87.6%. The result suggested that the activity of nitrite-oxidizing bacteria (NOB)

was completely inhibited in the PN-SBBR system, and nitrite was the main nitrogen species in the effluents after the biofilm formation. Additionally, TN removal efficiency in PN-SBBR was average about 61.2% at the same time, which was much higher than the conventional nitrogen removal via nitrate process (19.9%) reported in our previous literature (Wei et al., 2014a), suggesting that PN-SBBR could be used as an effective system for enhanced TN treatment, especially when treating wastewater with low COD/N ratio. The reason may be attributed to the presence of anoxic zone inside of the PN biofilm, which may cause the denitrification via nitrite path in aeration phase through the utilizing of insufficient carbon resource.

The achievement of PN-SBBR was accompanied by not only the changes in effluent quality, but also by the formation and generation of biofilm. The SBBR system was started-up by adding suspended activated sludge with a fluffy, irregular, loose morphology as seed sludge (Fig. S2A). After 10-days inoculation, it can be seen that a thin biofilm was easily attached onto the surface of bio-carrier (Fig. S2B). Afterwards, the biofilm thickness was generally developed in the system and therefore led to an increase in biomass concentration (Fig. S2C). Subsequently, biofilm entrapped inside the carrier continued to grow till to balance during the stable operation of PN-system (Fig. S2D), causing the biomass in each carrier was average about 0.14 g (n=3). At the end of study, the total amounts of biomass in suspended phase and attached carrier were 0.5 and 5.35 g/L, respectively, suggesting that the major portion of the biomass was attached onto the carrier in PN-system.

3.2 Variations of EPS contents during PN-SBBR achievement process

EPS production by attached microorganisms is considered as a very complicated process, which is affected by many operational parameters in the environment

(Czaczyk and Myszka, 2007). In present study, the main compositions of EPS, including PRO and PS, were measured and compared in the seed sludge and PN-biofilm. It was observed from Fig. 2 that both contents of PRO and PS in LB-EPS and TB-EPS were reduced after the achievement of PN-biofilm process. PRO and PS contents in TB-EPS were much higher than those in LB-EPS in both seed sludge and PN-biofilm, suggesting that TB-EPS was the main distribution and composition in the double-layered EPS. Yang and Li (2009) also found that LB-EPS have a relatively weak capacity to bind the floc constitutes. However, LB-EPS has been proved to play a significant role for influencing the flocculation, sedimentation and dewaterability of sludge, which is closely related to the sludge-water separation performance as specified by the ESS, SVI and SRT values (Li and Yang, 2007).

As shown in Fig. 2, PRO had about 4.8-20.3 times higher contents than those of PS for both kinds of EPS fractions, and the abundance of PRO may be attributed to the presence of a large quantity of exoenzymes in sludge (Fr et al., 1995). After the achievement of PN-SBBR, PS and PN contents decreased by 66.5% and 32.1% in LB-EPS, and by 72.2% and 36.2% in TB-EPS, respectively. The result suggested that PS contents were varied significantly in the attachment of activated sludge to bio-carrier for microbial biofilm formation. Additionally, TB-EPS contents decreased much higher degree than those in LB-EPS, suggesting that TB-EPS likely played a significant role for cell attachment.

Generally, the two kinds of EPS fractions play different roles in affecting the properties of microbial aggregates in the flied of wastewater treatment, including adsorption ability, flocculation ability, dewatering and stability etc. It was found that

LB-EPS increased significantly to environmental stress (such as low DO, salinity and toxic compound etc) than that of TB-EPS, which may be attributed to LB-EPS in the outer layer acted as the first place at which the biofilm has contact and interacts with toxic compound (You et al., 2015). Wang et al. (2013) evaluated the effect of salinity on EPS fractions of activated sludge in an anoxic-aerobic SBR, indicating that the PS in the LB-EPS is more sensitive to salinity variation than that in the TB-EPS. Zhang et al. (2011) also reported the different characteristics of EPS fractions in a PN-biofilm system, suggesting that a clear release of PS in the LB-EPS fraction was detected during the enhancement of salinity. Moreover, LB-EPS showed stronger binding properties to metallic cations ($Zn^{2+}$and Co^{2+}) than TB-EPS, and the main chemical groups involved in the interactions between contaminants were apparently alcohol, carboxyl and amino (Sun et al., 2009). However, TB-EPS exhibited a higher flocculating ability than that of LB-EPS, which could be attributable to high contents of macromolecules (330-1200 kDa) and trivalent cations. (Yu et al. 2009).

3.3 Fluorescence spectra of LB-EPS and TB-EPS

Fig. 3 shows the EEM spectra of LB-EPS and TB-EPS extracted from seed sludge and PN-biofilm on day 1 and day 90. Table 1 summarizes the fluorescent peak location and intensity of 3D-EEM spectra from the two types of EPS fractions. As shown in Fig. 3, three fluorescent peaks (A, B and C) were obviously observed, suggesting that LB-EPS and TB-EPS had similar chemical compositions regardless of seed sludge and PN-biofilm. Peak A and B were located at Ex/Em wavelengths of 289-290/352-360.5 nm and 230/331-360 nm, respectively, relating to the presence of

aromatic protein-like and tryptophan protein-like substances (Sheng and Yu, 2006). Peak C was indentified at Ex/Em of 350-360/432.5-447 nm, corresponding to the presence of humic acid-like substances (Wei et al., 2015b). It was also found that the fluorescent intensities of LB-EPS and TB-EPS in seed sludge were significantly higher than those in PN-biofilm. Peak A, B and C were reduced to 19.5, 32.0, and 9.56 a.u. in LB-EPS, while those were 547.1, 458.4, 102.8 a.u. in TB-EPS, respectively. Furthermore, there was a slight blue shift in term of emission in TB-EPS, implying the changed chemical structure of fluorophore-related functional groups during the biofilm formation process.

Synchronous fluorescence spectra have been developed as an elegant approach to resolve the problem of spectral overlapping problem (Sanchez et al., 1990). Fig. S3 displays the synchronous fluorescence spectra of two types of EPS from seed sludge and PN-biofilm. The whole wavelength in synchronous fluorescence spectra could be divided into three ranges of 250-300, 300-380 and 380-550 nm, assigning to the presence of protein-like, fulvic-like, and humic-like fluorescence fractions, respectively (Wei et al., 2016). It was obviously observed that the both LB-EPS and TB-EPS in PN-biofilm had higher fluorescent intensities than those of seed sludge. Moreover, a much higher fluorescent intensity was observed at 285 nm than other two kinds of fractions, suggesting that the protein-like fraction was the predominant component in EPS, as similarly with the result of chemical and EEM analysis. Therefore, synchronous fluorescence spectra could be used as a useful method for EPS characterization.

3.4 Typical cycle of PN-SBBR

Fig. 4 shows the time-course of nitrogen species and control parameters in a typical PN-SBBR cycle during stable operation. It was found from Fig. 4A that NH_4^+-N concentration was quickly reduced from 204.7 to 107.8 mg/L due to the dilution process after the influent addition (0-5 min), and generally changed to 91.0 mg/L during the anoxic denitrification phase (5-90 min). The reason of decreased NH_4^+-N concentration may be attributed to biosorption process. Correspondingly, both NO_2^--N and NO_3^--N were used as electron acceptor for pre-denitrification phase, and their concentrations decreased from 68.7 and 5.49 mg/L to 0.86 and 1.38 mg/L, respectively. Meanwhile, the pH values increased from 8.99 to 9.52 at the same time, as displayed in Fig. 4B.

During the subsequently aeration phase (90-450 min), NH_4^+-N concentration generally decreased from 91.0 to 0.80 mg/L, and the effluent NH_4^+-N removal efficiency was high of 99.6%. As a time control parameter for nitrogen removal, the pH value in PN system generally decreased from 9.52 to 8.93 in nitrification process by consuming alkalinity, and next slightly increased to 9.01 due to air stripping of CO_2 from the system (Fig. 4B). Although the DO concentration was always about 4 mg/L during aeration phase, it was obvious observed the nitrite accumulation with low nitrate production in the effluent of PN-SBBR system. More detailed, the NO_2^--N and NO_3^--N concentrations varied to 66.2 and 9.01 mg/L, respectively. Compared to conventional BNR process, no nitrite peak appeared during the whole cycle, suggesting that the activity of NOB was fully inhibited in PN-biofilm system.

High influent FA concentration has been successfully selected as the key control strategy for PN process achievement and maintenance, especially when treating

nitrogen-rich and high pH value wastewaters (Wei et al., 2014b). It is well accepted that NOB are more sensitive to the presence of FA than that of ammonia-oxidizing bacteria (AOB). Anthonisen et al (1976) found that FA concentration could inhibit *Nitrosomonads* and *Nitrobcaters* in the ranges of 10-150 and 0.1-1.0 mg/L, respectively. It was found from Fig. S4 that the FA concentration was high of 73.6 mg/L after the influent wastewater pumped into the reactor (5 min). Although FA concentration was generally reduced to 3.7 mg/L due to the ammonium oxidation to nitrite at 390 min, it was still much higher than the reported inhibitory level (0.1-1.0 mg/L) of NOB. Therefore, nitrite accumulation obviously occurred in the PN-biofilm system during the aeration phase (Fig. 4A). Additionally, when FA concentration decreased to 0.41 mg/L, NO_3^--N concentration rapidly increased from 4.31 to 9.01 mg/L, causing NAR decreased from 93.0% at 390 min to 88.0% at 450 min. The phenomenon further proved the inhibitory effect of FA on the activity of NOB for the oxidation of nitrite. Meanwhile, the FNA concentration was always at low level (less than 0.0006 mg/L), which was much lower than the reported inhibitory levels of nitrifying organisms (0.22-2.8 mg/L). Therefore, in present study, FA played a significant role on the inhibition activity of NOB and the occurrence of nitrite accumulation.

3.5 Greenhouse gas emission of PN-SBBR system

Fig. 5 shows N_2O and CO_2 emission rates during a typical cycle in PN-biofilm system. It was found that CO_2 had much higher emission rate than that of N_2O throughout of the whole cycle. The maximum value of CO_2 emission rate was high of 64.6 μg/min at 330 min, which was about 4.58 times higher than that of anoxic phase. The CO_2 emission amounts were 2.7 and 65.0 mg in aeration phase and anoxic phase, respectively, causing a total of 67.7 mg CO_2 emission per cycle. It is generally

accepted that organic matter oxidation and alkalinity consumption are the two principal sources of CO_2 production during wastewater treatment (Daigger et al., 2004). When the biodegradable organic matter is stabilized by aerobic treatment, the carbon in the organic matter is converted to CO_2. The other principal source of CO_2 production is alkalinity consumption from nitrification, which results in the conversion of inorganic carbon to CO_2.

As shown in Fig. 5, the N_2O emission rate during the whole cycle displayed a similar tendency with CO_2. It is well accepted that N_2O emission from biological wastewater treatment may be attributed to two possible pathways: autotrophic nitrification and heterotrophic denitrification (Law et al., 2012). The N_2O emission rate was always low throughout of anoxic phase (less than 3 μg/min), and the majority of N_2O was produced from aeration phase. The reason of a relatively higher N_2O emission rate in the initial 30 min may be attributed to the reminding NO_2^--N in the previous cycle. The maximum N_2O emission rates in anoxic phase and aeration phase were 2.52 and 29.9 μg/min at 30 and 240 min, respectively. As a result, the total N_2O emission amount per cycle from PN-SBBR system was 16.5 mg, which was approximate 4.79% of removed nitrogen.

4. Conclusions

In summary, PN process was successfully achieved and maintained in a SBBR for treating high ammonia wastewater. High NH_4^+-N removal efficiency and NAR were observed after PN-biofilm achievement. 3D-EEM and synchronous fluorescence spectra implied the similar chemical compositions LB-EPS and TB-EPS from seed sludge and PN-bioflim. The cycle data suggested that the majority of CO_2 and N_2O were produced from aeration phase, and their total emission amounts per cycle were

67.7 and 16.5 mg, respectively. The GHG emission result is valuable for understanding the process of nitrogen removal via nitrite in a biofilm system.

5. Acknowledgements

This study was supported by the Natural Science Foundation of Chinese Province (21377046), Special project of independent innovation and achievements transformation of Shandong Province (2014ZZCX05101), Science and technology development plan project of Shandong province (2014GGH217006), and QW thanks the Special Foundation for Taishan Scholar Professorship of Shandong Province and UJN (No.ts20130937).

References

1. Adav, S.S., Lee, D.J., Lai, J.Y. 2009. Biological nitrification-denitrification with alternating oxic and anoxic operations using aerobic granules. Appl. Microbiol. Biotechnol. 84, 1181-1189.
2. Anthonisen, A.C., Srinath, E.G. 1976. Inhibition of Nitrification by Ammonia and Nitrous-Acid. J. Water Pollut. Control. Fed. 48, 835-52.
3. APHA, AWWA, WEF. 2005. Standards methods for the examination of water and wastewater. 21st ed. Washington, D.C
4. Chen, Z., Wang, X., Yang, Y.Y., Jr, M.W.M., Yuan, Y. 2016. Partial nitrification and denitrification of mature landfill leachate using a pilot-scale continuous activated sludge process at low dissolved oxygen. Bioresour. Technol. 218, 580-588.
5. Czaczyk, K., Myszka, K. 2007. Biosynthesis of Extracellular Polymeric Substances (EPS) and Its Role in Microbial Biofilm Formation. Pol J Environ Stud. 16, 799-806.
6. Daigger, G., Peterson, R., Witherspoon, J., Allen, E. 2004. Impact of global warming concerns on wastewater treatment plant design and operation. in: advances in water and wastewater treatment. ASCE Publications. 1-19.
7. Ford, D.L., Kachtick, J.W. 1980. Comprehensive Analysis of Nitrification of Chemical Processing Wastewaters. J. Water Pollut. Control. Fed. 52, 2726-2746.
8. Fr, B., Griebe, T., Nielsen, P. 1995. Enzymatic activity in the activated-sludge floc matrix. Appl. Microbiol. Biotechnol. 43, 755-761.
9. Ge, S., Peng, Y., Shuang, Q., Ao, Z., Ren, N. 2014. Complete nitrogen removal from municipal wastewater via partial nitrification by appropriately alternating anoxic/aerobic conditions in a continuous plug-flow step feed process. Water Res. 55, 95-105.
10. Gilbert, E.M., Agrawal, S., Karst, S.M., Horn, H., Nielsen, P.H., Lackner, S. 2014. Low temperature partial nitritation/anammox in a moving bed biofilm reactor treating low

strength wastewater. Environ. Sci. Technol. 48, 8784-8792.
11. Hosseini, S.H., Borghei, S.M. 2005. The treatment of phenolic wastewater using a moving bed bio-reactor. Process Biochem. 40, 1027-1031.
12. Hu, Z., Zhang, J., Xie, H., Liang, S., Wang, J., Zhang, T. 2011. Effect of anoxic/aerobic phase fraction on N_2O emission in a sequencing batch reactor under low temperature. Bioresour. Technol. 102, 5486-5491.
13. Jin, Y., Ding, D., Feng, C., Tong, S., Suemura, T., Zhang, F. 2012. Performance of sequencing batch biofilm reactors with different control systems in treating synthetic municipal wastewater. Bioresour. Technol. 104, 12-8.
14. Kampschreur, M.J., Temmink, H., Kleerebezem, R., Jetten, M.S., van Loosdrecht, M. 2009. Nitrous oxide emission during wastewater treatment. Water Res. 43, 4093-4103.
15. Kong, Q., Wang, Z.B., Niu, P.F., Miao, M.S. 2016. Greenhouse gas emission and microbial community dynamics during simultaneous nitrification and denitrification process. Bioresour. Technol. 210, 94-100.
16. Law, Y., Ye, L., Pan, Y., Yuan, Z. 2012. Nitrous oxide emissions from wastewater treatment processes. Philos T R Soc B. 367, 1265-1277.
17. Li, H., Shaobin, H., Shaofeng, Z., Pengfei, C., Yongqing, Z. 2016. Study of extracellular polymeric substances in the biofilms of a suspended biofilter for nitric oxide removal. Appl. Microbiol. Biotechnol. 100, 1-11.
18. Li, X.Y., Yang, S.F. 2007. Influence of loosely bound extracellular polymeric substances (EPS) on the flocculation, sedimentation and dewaterability of activated sludge. Water Res. 41, 1022-30.
19. Liu, X.M., Sheng, G.P., Luo, H.W., Zhang, F., Yuan, S.J., Xu, J., Zeng, R.J., Wu, J.G., Yu, H.Q. 2010. Contribution of extracellular polymeric substances (EPS) to the sludge aggregation. Environ. Sci. Technol. 44, 4355-60.
20. Peng, Y., Zhu, G. 2006. Biological nitrogen removal with nitrification and denitrification via nitrite pathway. Appl. Microbiol. Biotechnol. 73, 15-26.
21. Qiao, S., Kawakubo, Y., Koyama, T., Furukawa, K. 2008. Partial nitritation of raw anaerobic sludge digester liquor by swim-bed and swim-bed activated sludge processes and comparison of their sludge characteristics. J. Biosci. Bioeng. 106, 433-441.
22. Sanchez, F.G., Rubio, A.L.R., Blanco, C.C., Suarez, R.S. 1990. Three-dimensional synchronous fluorescence spectrometry for the analysis of three-component alkaloid mixtures. Talanta. 37, 579-584.
23. Sheng, G.P., Yu, H.Q. 2006. Characterization of extracellular polymeric substances of aerobic and anaerobic sludge using three-dimensional excitation and emission matrix fluorescence spectroscopy. Water Res. 40, 1233-9.
24. Shi, X.Y., Yu, H.Q., Sun, Y.J., Xia, H. 2009. Characteristics of aerobic granules rich in autotrophic ammonium-oxidizing bacteria in a sequencing batch reactor. Chem. Eng. J. 147, 102-109.
25. Sun, X.F., Wang, S.G., Zhang, X.M., Chen, J.P., Li, X.M., Gao, B.Y., Ma, Y. 2009. Spectroscopic study of Zn^{2+} and Co^{2+} binding to extracellular polymeric substances (EPS) from aerobic granules. J. Colloid. Interf. Sci. 335, 11-17.
26. Wang, C.C., Lee, P.H., Kumar, M., Huang, Y.T., Sung, S., Lin, J.G. 2010. Simultaneous partial nitrification, anaerobic ammonium oxidation and denitrification (SNAD) in a full-scale

landfill-leachate treatment plant. J. Hazard. Mater. 175, 622-628.

27. Wei, D., Dong, H., Wu, N., Ngo, H.H., Guo, W., Du, B., Wei, Q. 2016. A Fluorescence Approach to Assess the Production of Soluble Microbial Products from Aerobic Granular Sludge Under the Stress of 2,4-Dichlorophenol. Sci rep. 6, 24444
28. Wei, D., Du, B., Zhang, J., Hu, Z., Liang, S., Li, Y. 2015a. Composition of extracellular polymeric substances in a partial nitrification reactor treating high ammonia wastewater and nitrous oxide emission. Bioresour. Technol. 190, 474-479.
29. Wei, D., Shi, L., Zhang, G., Wang, Y., Shi, S., Wei, Q., Du, B. 2014a. Comparison of nitrous oxide emissions in partial nitrifying and full nitrifying granular sludge reactors treating ammonium-rich wastewater. Bioresour. Technol. 171, 487-490.
30. Wei, D., Wang, B., Ngo, H.H., Guo, W., Han, F., Wang, X., Du, B., Wei, Q. 2015b. Role of extracellular polymeric substances in biosorption of dye wastewater using aerobic granular sludge. Bioresour. Technol. 185, 14-20.
31. Wei, D., Xue, X., Yan, L., Sun, M., Zhang, G., Shi, L., Du, B. 2014b. Effect of influent ammonium concentration on the shift of full nitritation to partial nitrification in a sequencing batch reactor at ambient temperature. Chem. Eng. J. 235, 19-26.
32. Wang, Z., Gao, M., Wang, Z., She, Z., Chang, Q., Sun, C., Zhang, J., Ren, Y., Yang, N. 2013. Effect of salinity on extracellular polymeric substances of activated sludge from an anoxic-aerobic sequencing batch reactor. Chemosphere. 93, 2789-2795.
33. Yang, S.F., Li, X.Y. 2009. Influences of extracellular polymeric substances (EPS) on the characteristics of activated sludge under non-steady-state conditions. Process Biochem. 44, 91-96.
34. Yin, J., Zhang, P., Li, F., Li, G., Hai, B. 2015. Simultaneous biological nitrogen and phosphorus removal with a sequencing batch reactor–biofilm system. Int. Biodeterior. Biodegrad. 103, 245-261.
35. You, G., Hou, J., Xu, Y., Wang, C., Wang, P., Miao, L., Ao, Y., Li, Y., Lv, B. 2015. Effects of CeO_2 nanoparticles on production and physicochemical characteristics of extracellular polymeric substances in biofilms in sequencing batch biofilm reactor. Bioresour. Technol. 194, 91-98.
36. Yu, G.H., He, P.J., Shao, L.M. 2009. Characteristics of extracellular polymeric substances (EPS) fractions from excess sludges and their effects on bioflocculability. Bioresour. Technol. 100, 3193-3198.
37. Zhang, L., Liu, J., Liu, C., Zhang, J., Yang, J. 2016. Performance of a fixed-bed biofilm reactor with microbubble aeration in aerobic wastewater treatment. Water Sci. Technol. 74, 138-146.
38. Zhang, Z.J., Chen, S.H., Wang, S.M., Luo, H.Y. 2011. Characterization of extracellular polymeric substances from biofilm in the process of starting-up a partial nitrification process under salt stress. Appl. Microbiol. Biotechnol. 89, 1563-1571.
39. Zhao, W., Yang, S., Huang, Q., Peng, C. 2015. Bacterial cell surface properties: Role of loosely bound extracellular polymeric substances (LB-EPS). Colloids Surf B: Biointerfaces. 128, 600-607.

Figure Captions

Fig. 1 Overall performance of PN-SBBR during the whole operation: (A) Influent and effluent NH_4^+-N concentrations, and removal efficiencies; (B) Effluent NO_2^--N and NO_3^--N concentrations.

Fig. 2 Changes in LB-EPS and TB-EPS contents during the PN-SBBR achievement process.

Fig. 3 EEM spectra of LB-EPS and TB-EPS extracted from seed sludge and PN-biofilm: (A) LB-EPS and (B) TB-EPS from seed sludge; (C) LB-EPS and (D) TB-EPS from PN-biofilm.

Fig. 4 Time-course of nitrogen species and control parameters in a typical PN-SBBR cycle during stable operation: (A) NH_4^+-N, NO_2^--N and NO_3^--N concentrations; (B) pH and DO values.

Fig. 5 N_2O and CO_2 emission rates during a typical cycle in PN-biofilm system.

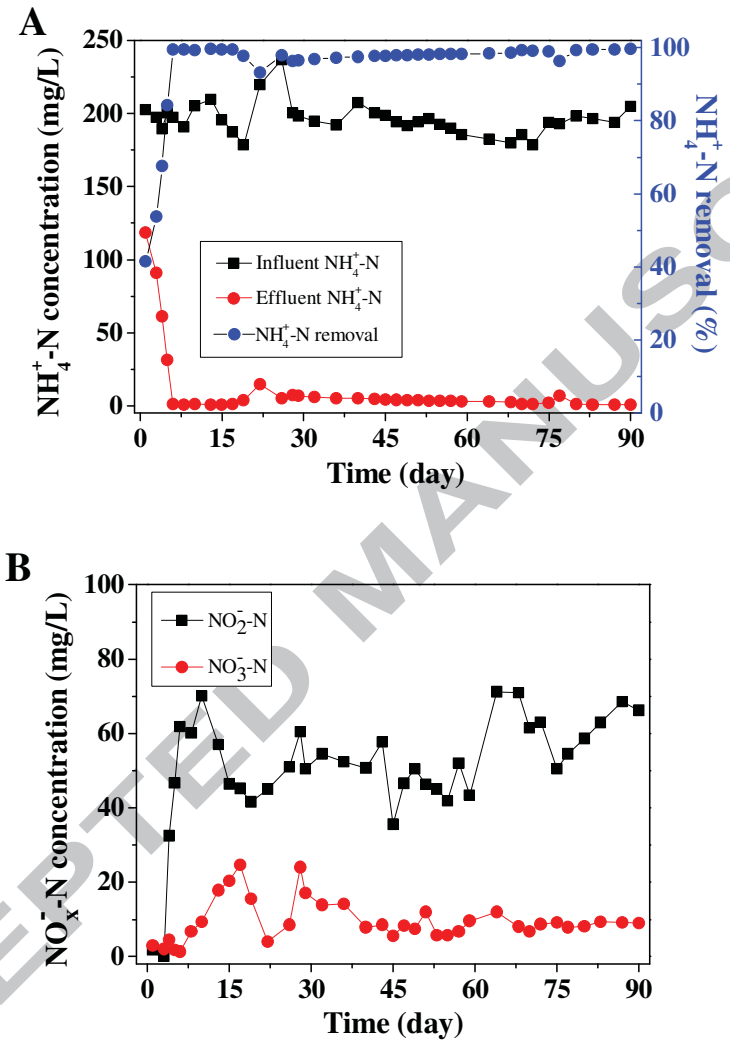

Fig. 1 Overall performance of PN-SBBR during the whole operation: (A) Influent and effluent NH_4^+-N concentrations, and removal efficiencies; (B) Effluent NO_2^--N and NO_3^--N concentrations.

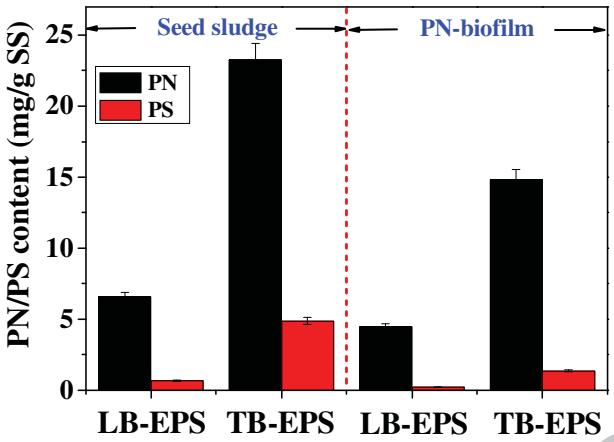

478

479 **Fig. 2** Changes in LB-EPS and TB-EPS contents during the PN-SBBR achievement

480 process.

481

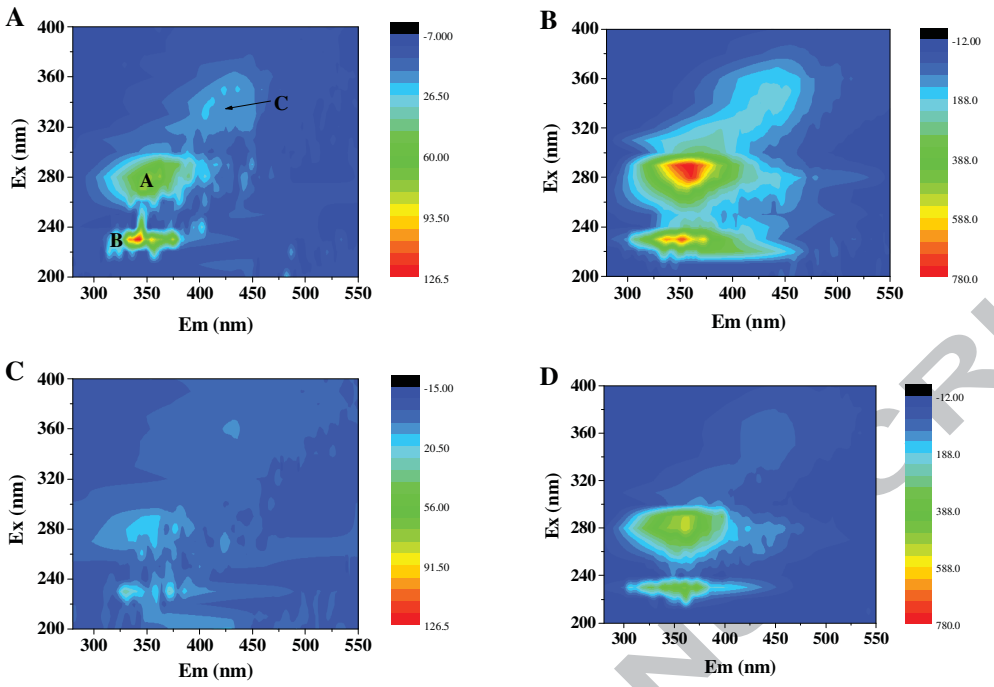

482 **Fig. 3** EEM spectra of LB-EPS and TB-EPS extracted from seed sludge and
483 PN-biofilm: (A) LB-EPS and (B) TB-EPS from seed sludge; (C) LB-EPS and (D)
484 TB-EPS from PN-biofilm.
485

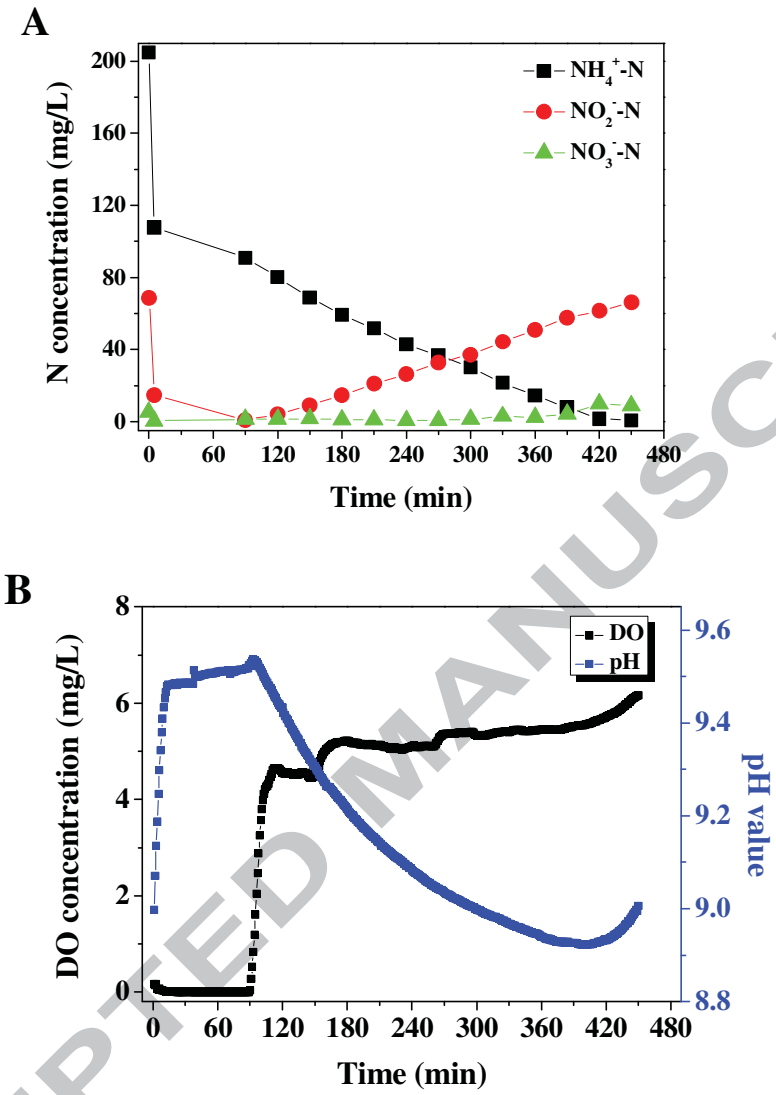

Fig. 4 Time-course of nitrogen species and control parameters in a typical PN-SBBR cycle during stable operation: (A) NH_4^+-N, NO_2^--N and NO_3^--N concentrations; (B) pH and DO values.

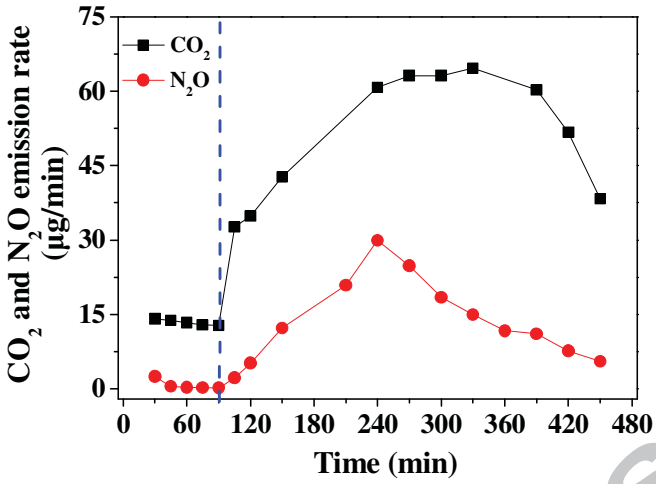

491

492 **Fig. 5** N_2O and CO_2 emission rates during a typical cycle in PN-biofilm system.

493

494

495

496

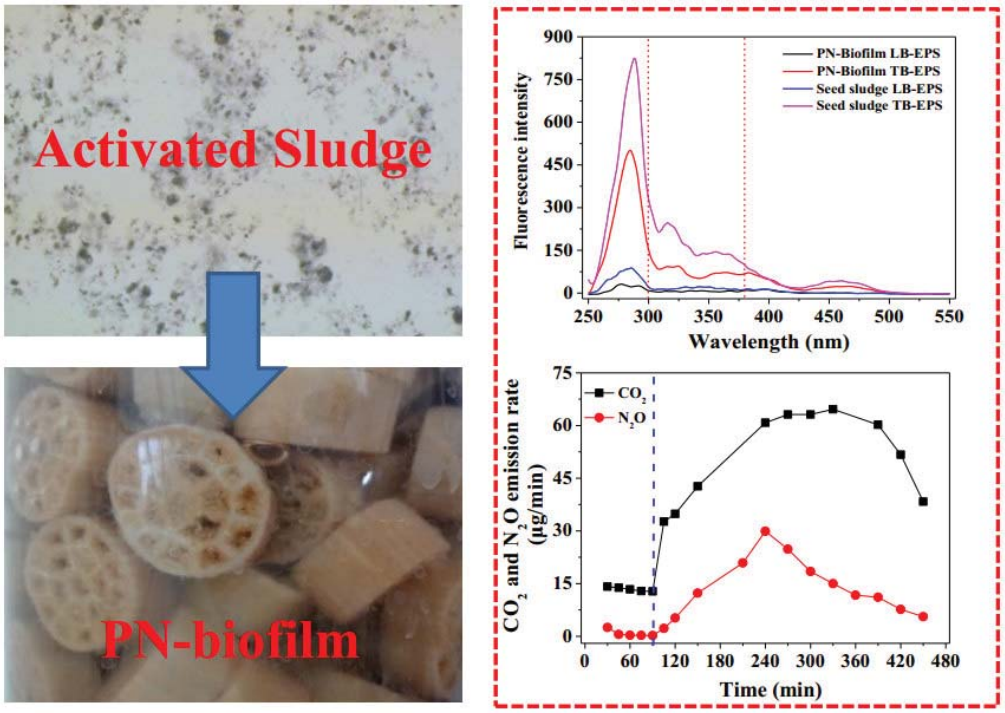

497

498

499

500

501 **Table 1** Fluorescence spectral parameters of LB-EPS and TB-EPS samples extracted
502 from seed sludge and PN-biofilm.

Simples	Simples	Peak A		Peak B		Peak C	
		Ex/Em	Intensity	Ex/Em	Intensity	Ex/Em	Intensity
seed sludge	LB-EPS	280/352	81.9	230/342	126.4	350/436	21.3
	TB-EPS	290/360	779.2	230/351.5	719.4	350/434	207.9
PN biofilm	LB-EPS	280/354	19.5	230/331	32.0	360/432.5	9.56
	TB-EPS	280/360.5	547.1	230/360	458.4	350/447	102.8

503
504

505

506

507 **Highlights**

508 ➢ Partial nitrification was successfully achieved and maintained in a SBBR.

509 ➢ PN and PS contents were reduced during the achievement of PN process.

510 ➢ 3D-EEM implied that LB-EPS and TB-EPS had similar chemical compositions.

511 ➢ CO_2 and N_2O emission amounts per cycle were 67.7 mg and 16.5 mg.

512